Rev.Adv.Mater.Sci. 25 (2010) 99-106

EFFECT OF A SCANDIUM ADDITION ON AN Al-2% Si ALLOY PROCESSED BY ECAP

K. Venkateswarlu[1], V. Rajinikanth[2], Ajoy Kumar Ray[2], Cheng Xu[3,4] and Terence G. Langdon[3,5]

[1]Materials Science Division, National Aerospace Laboratories (CSIR), Bangalore- 560017, India
[2]National Metallurgical Laboratory (CSIR), Jamshedpur - 831007, India
[3]Departments of Aerospace & Mechanical Engineering and Materials Science, University of Southern California, Los Angeles, CA 90089-1453, USA
[4] Now with Ningbo Institute of Materials Technology and Engineering, Chinese Academy of Sciences, Ningbo, Zhejiang 315201, P.R. China
[5]Materials Research Group, School of Engineering Sciences, University of Southampton, Southampton SO17 1BJ, U.K.

Received: December 04, 2009

Abstract. Two alloys, Al-2% Si and Al-2% Si-0.25% Sc, were subjected to equal-channel angular pressing (ECAP) up to a maximum of 4 passes using route B_c at room temperature. This processing gave ultrafine-grained microstructures with grain sizes of ~0.70 μm without Sc and ~0.30 μm with the 0.25% Sc addition. The improvement in the mechanical properties of the Al–2% Si alloy due to the Sc addition was studied using a ball-indentation technique (BIT). These tests showed that the addition of 0.25% Sc decreased the grain size of the Al-2% Si alloy in the cast condition from 40 to 25 μm with an increase in the ultimate tensile strength (UTS) from ~106 to ~185 MPa. In addition, ECAP of the Al-2% Si-0.25% Sc alloy gave a UTS of ~355 MPa which was ~30% higher than the Al-2% Si alloy without the Sc addition. This increase is due to the presence of fine Al_3Sc precipitates.

1. INTRODUCTION

The density of Si is 2.3 g/cm^3 and Al is 2.7 g/cm^3 and therefore Si is one of the few elements which can be alloyed to Al without any loss of the light-weight advantage. In addition, the low coefficient of thermal expansion, high wear resistance and fluidity, which are characteristic of Al-Si alloys, have led to these alloys receiving considerable interest as candidate materials for automotive and aerospace applications [1,2]. Therefore, Al-Si alloys are attractive in a large number of applications in the automobile industries such as for pistons, cylinder blocks and liners [3,4]. In practice, higher silicon content is responsible for superior tribological properties. However, these alloys exhibit low strength and ductility properties. Attempts are now underway to improve their strength properties by the addition of alloying elements like copper and magnesium followed by quenching and ageing.

An effective alternative method for increasing the strength of Al alloys, first proposed by Willey in 1971 [5], involves the addition of scandium as an alloying element. In practice, the Al–Sc solid solution de-

Corresponding author: K. Venkateswarlu, e-mail: kvenkat@nal.res.in

composes to form a fine dispersion of homogeneously nucleated, equilibrium precipitates of a stable $L1_2$ phase, Al_3Sc, with a lattice parameter mismatch of 1.6%, and this can produce a significant ageing response despite the relatively low solubility of Sc and hence a lower volume fraction [6–11]. The Sc serves as a potent grain refiner in castings, particularly when used in combination with Zr [12–15]. It has been shown that a grain size of 40–45 μm in Al is only possible when the Sc addition exceeds 0.6 wt.%. The presence of various shapes of Al_3Sc particles including its finer precipitates is responsible for a good grain-refining efficiency. Experiments showed that a fine-grained structure of Al in the range of 40–45 μm with an Sc addition was responsible for higher wear resistance values as compared to an Al alloy having a grain size of 120–130 μm prepared by adding commercial grain refiners such as TiBAl [16]. As a result, it was found that Sc additions to Al alloys improve the mechanical properties by decreasing the grain size.

A further improvement in mechanical properties can be achieved by employing a severe plastic deformation (SPD) processes such as equal-channel angular pressing (ECAP) [17]. The ECAP route has been considered as one of the most efficient SPD processes where substantial grain refinement leads to significant strengthening properties [18-21]. Among various route available in the ECAP technique, route B_c where the sample is rotated by 90° between each pass [22] was selected for this investigation because it was established earlier that this is the optimum processing route for achieving a homogeneous microstructure containing a large fraction of boundaries having high angles of misorientation [23]. Moreover, attempts are made to incorporate ECAP in the processing of metal sheets and plates [24].

The present investigation involves the addition of a minor quantity of Sc (0.25 wt.%) to an Al-2% Si alloy in order to understand the influence of Sc and subsequently to process these two alloys (Al-2% Si and Al-2% Si-0.25% Sc) by equal channel angular pressing (ECAP) using route B_c at room temperature. The mechanical properties of the as-cast and ECAP processed alloys were evaluated using the ball-indentation technique and the mechanical properties of the Al-2% Si-0.25% Sc alloy was compared with earlier studies [25].

2. EXPERIMENTAL METHODS

The Al-2% Si alloy was prepared by a liquid metallurgy route by adding the required quantity of Si to Al, melting in an electrical resistance furnace at ~850 °C and pouring in a graphite mould of 12.5 mm diameter and 80 mm length. Before pouring in to the mould, care was taken to remove the entrapped gasses in the liquid Al by adding 1wt. % hexachloroethane. Similarly, an Al-2% Sc master alloy was added to an Al-2% Si melt in the appropriate quantity to finally yield an Al-2% Si-0.25% Sc alloy. The reasons for considering a low Si content in the experimental Al-Si alloy is that higher silicon contents will significantly damage the ECAP die during pressing and to ease the processing of this alloy using route B_c at room temperature. Many researchers have attempted to study the influence of straining these high silicon-containing Al alloys using processes like rotary die extrusion and ECAP using other processing routes. However, these other processes are not as effective by comparison with ECAP using route B_c. Finally, samples of 10 mm diameter and 60 mm length for ECAP were machined from the as-cast alloy. In order to carry out the ECAP successfully, a solid die was used with an internal channel of 10 mm in diameter bent through an abrupt angle of $\Phi = 90°$ and with an outer arc of curvature at the point of intersection of the two parts of the channel of $\Psi = 20°$. It can be shown from first principles that these values of Φ and Ψ lead to an imposed strain of ~1 on each pass through the die [26]. Since the number of ECAP passes using route B_c has been optimized to 4 [27,28], equivalent to an imposed strain of ~4, the present investigation was also limited to a total of 4 passes. It was found that processing by route B_c gave a homogeneous microstructure after 4 passes.

The mechanical properties of the ECAP samples were evaluated by both conventional tensile testing and using the ball-indentation technique (BIT). For conventional tensile testing, samples were prepared with gauge lengths of 4 mm along the pressing direction and cross-sectional areas of 3 mm × 2 mm. These tensile samples were pulled at room temperature at three different strain rates in the range from$1.0{\cdot}10^{-3}$ to $1.0{\cdot}10^{-1}$ s^{-1}. For BIT testing, a smaller sample with typical dimensions of 5 mm × 5 mm × 2 mm was sufficient and the load was applied from a selected height and repetitive loadings were performed through a loading–unloading–reloading sequence in order to establish multiple load–deflection curves. The experimental procedure for the BIT testing was discussed in detail elsewhere [29,30]. A detailed microstructural examination of both the as-cast and the ECAP samples was carried out by light microscopy, electron microscopy (SEM and TEM) and atomic force microscopy (AFM).

Table 1. Metallurgy of experimental alloys.

Alloy	*Chemical composition*, %				*Bulk Hardness*, *Hv*	*Grain Size*, μm
	Si	Fe	Sc	Al		
Al-2Si	2.16	0.14	-	Balance	37	40
Al-2Si-0.25Sc	2.05	0.12	0.23	Balance	57	25

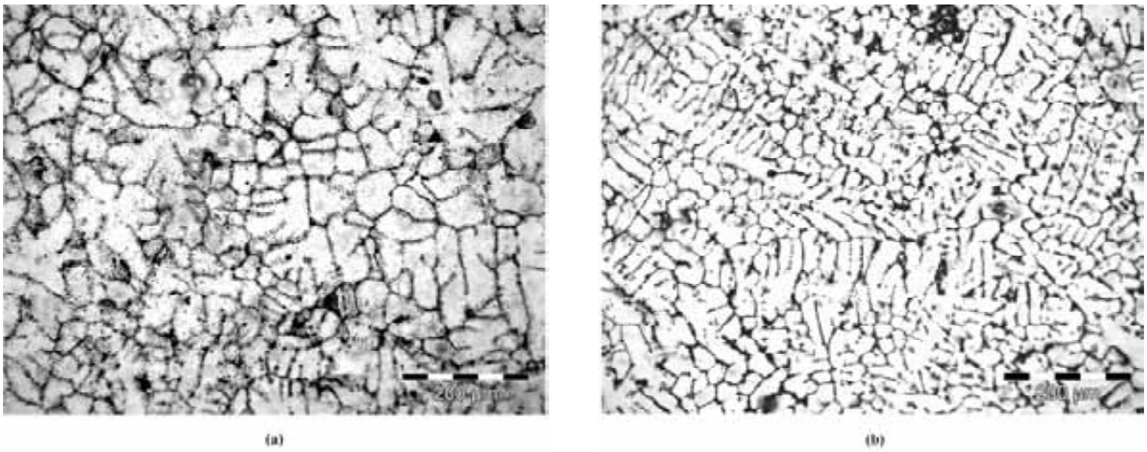

Fig. 1. Light images of Al-2% Si alloy (a) without Sc and (b) with 0.25% Sc.

3. RESULTS AND DISCUSSION

3.1. Microstructural studies

Table 1 shows the chemical composition, grain size and hardness values for the Al-2% Si and Al-2% Si-0.25% Sc alloys.

Figs. 1a and 1b show the light images of the Al-2% Si and Al-2% Si-0.25% Sc alloys, respectively. In Fig. 1a, it can be clearly seen that the finer Si particles of ~12 mm are uniformly distributed in the Al matrix. Fig. 1b shows a significant grain refinement due to the addition of 0.25% Sc as compared to the as-cast Al-2% Si alloy. The average grain sizes of the as-cast Al-2% Si and Al-2% Si-0.25% Sc alloys were ~40 and ~25 μm, respectively, measured by the linear intercept method. The formation of a smaller grain structure with the addition of Sc was due to the formation of intermetallic particles of the $L1_2$ type Al_3Sc phase in the Al melt which acted as heterogeneous nucleation sites during solidification. Also, due to the similarities between the crystal structures of the α-Al and Al_3Sc phases, the heterogeneous nucleation of α-Al might be expected to guide the epitaxial growth of α-Al on the $L1_2$ type Al_3Sc particles [31].

Most of the Si particles were at grain boundary networks as shown in the SEM image of the Al-2% Si-0.25% Sc alloy in Fig. 2. The improvement in properties of the Al-2% Si alloy due to the Sc addition was also reflected in the hardness values. The hardness due to the Sc addition in the Al-2% Si alloy increased from 37 to 57 Hv with the expected decrease in grain size as shown in Table 1. Fig. 3a shows the AFM image in topographic mode for the Al-2% Si-0.25% Sc alloy in which Si particles are

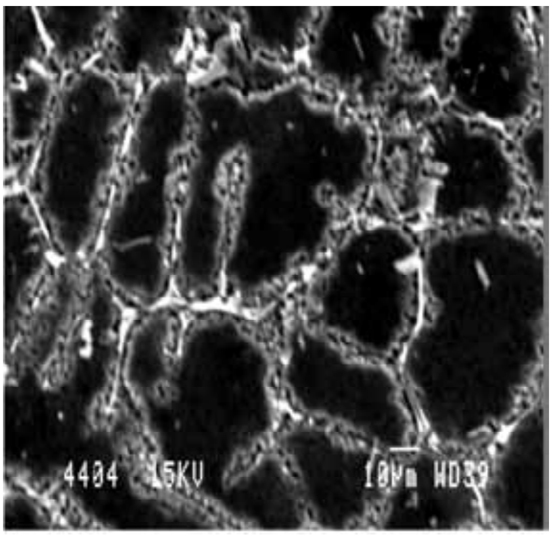

Fig. 2. SEM image of Al-2% Si-0.25% Sc alloy.

evenly distributed in the Al matrix. Fig. 3b shows the detailed topography of the surface where a 10 × 10 μm^2 area is considered and it shows that the Si particles appear as white spikes along the Z-direction. The average Si particle size was ~12 μm as measured by image processing schemes such as contrast stretching and thresholding in Fig. 3c.

SEM examination was also carried out on ECAP Al-2% Si-0.25% Sc alloy samples processed through 1, 2, 3, and 4 passes, respectively. Fig. 4 shows an SEM image of the 4 pass sample where the grain boundary network of Si as seen in Fig. 2 is totally absent and the Si particles are instead very fine and evenly distributed in the Al matrix. The reduction in Si particle sizes with the increase in the number of ECAP passes in the Al-2% Si and Al-2% Si-0.25% Sc alloys is shown in Table 2.

During processing by ECAP, the grain size of Al is drastically reduced and the average size of the Si particles was significantly reduced and uniformly distributed in the Al matrix. However, from the SEM image in Fig. 4 it is not possible to measure the grain size. Therefore, TEM and AFM studies were carried out to determine the grain sizes of the ECAP alloys. Table 2 shows the reduction in Si particles due to ECAP in both the Al-2% Si and the Al-2% Si-0.25% Sc alloys. Table 2 also records the Si particle size reduction with increasing numbers of ECAP passes. The recorded value for the as-cast Al-2% Si alloy gave Si particles with a size of ~12 μm whereas ~11 μm was observed in the Al-2% Si-0.25% Sc alloy. There was a drastic reduction in the size of the Si particles from the as-cast condition to the 1 pass condition for both alloys but there was no change in size of the Si particles from 1 to 4

Table 2. Average size of Si particles after ECAP.

Condition	*Size of Si particles* (μm) Al-2Si alloy	Al-2Si-0.25Sc alloy
As cast	~12	~11
1 pass	~1.40	~1.40
2 pass	~1.34	~1.35
3 pass	~1.25	~1.21
4 pass	~1.08	~1.02

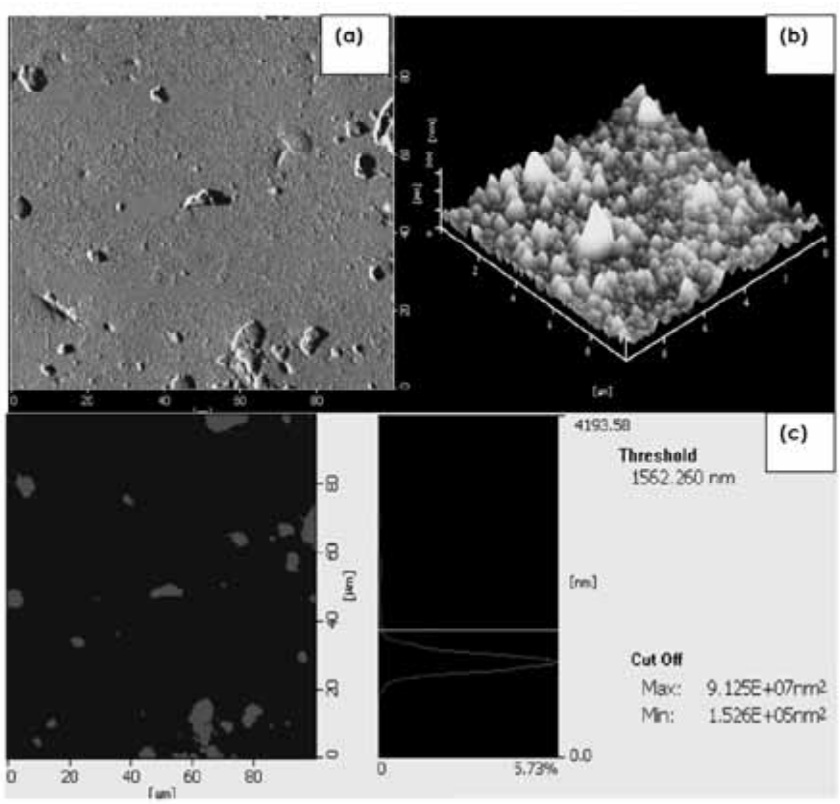

Fig. 3. AFM image of Al-2% Si-0.25% Sc alloy.

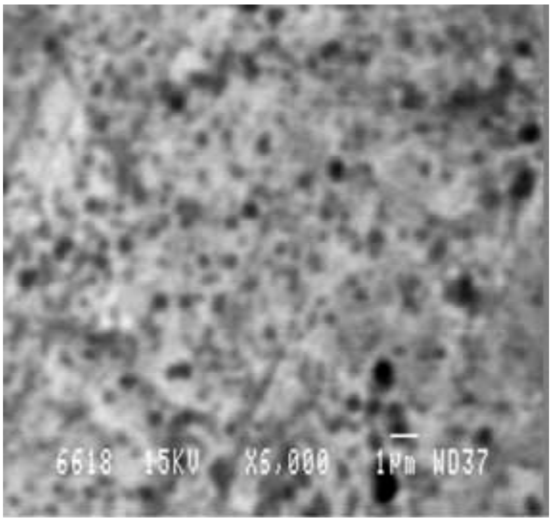

Fig. 4. SEM image of Al-2% Si-0.25% Sc alloy after 4 ECAP passes.

passes. In addition, the Si particle size reduction in the Al-2% Si-0.25% Sc alloy also showed similar results. Interestingly, it can be seen that the Sc addition does not affect the reduction in size of the Si particles in the Al-2% Si-0.25% Sc alloy during ECAP and the particle sizes are similar to the Al-2% Si alloy.

Fig. 5a and 5b shows that the grain sizes are refined to the sub-micrometer level during ECAP up to 4 passes for both the Al-2% Si and Al-2% Si-0.25% Sc alloys. The ultrafine grain sizes were ~700 nm in the Al-2% Si alloy and ~300 nm in the Al-2% Si-0.25% Sc alloy. It is also observed in Fig. 5b that Al_3Sc precipitates (indicated by arrows) in the range of 80-100 nm are uniformly distributed in the Al matrix. AFM studies clearly demonstrated that the grain size of the Al-2% Si alloy with the Sc addition was equiaxed after 4 ECAP passes with an ultrafine size of ~0.3 μm as shown in Fig. 6.

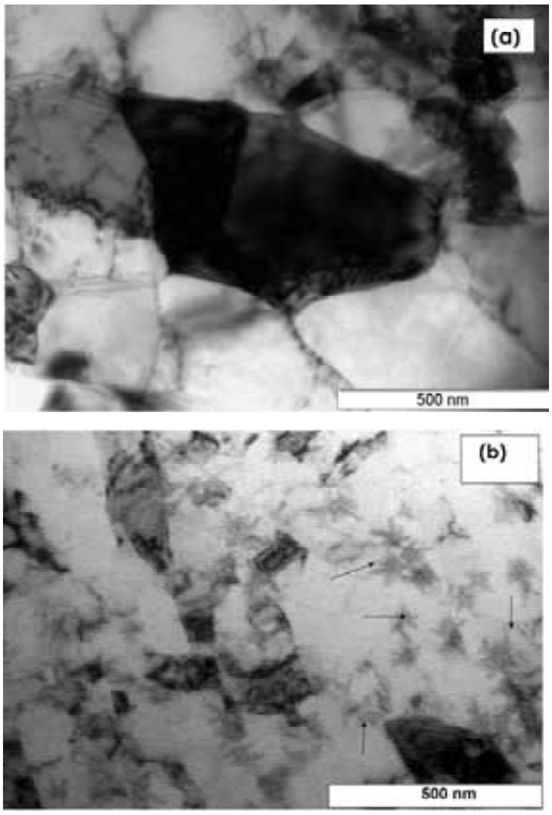

Fig. 5. TEM images of Al-2% Si alloy subjected to 4 passes (a) without Sc and (b) with 0.25% Sc (arrows show start type Al_3Sc precipitates).

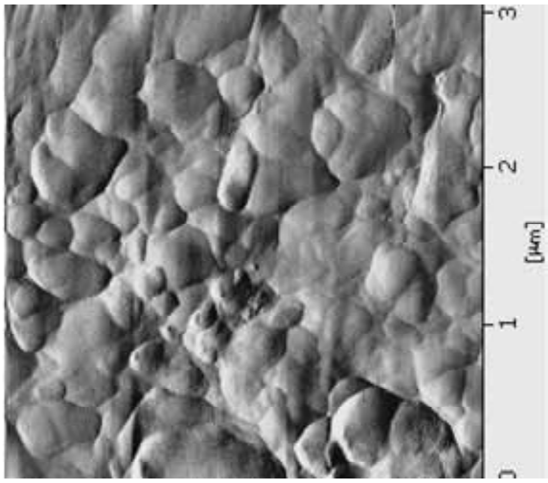

Fig. 6. AFM image of Al-2% Si-0.25% Sc alloy showing the average grain size of ~0.30 μm.

3.2. Tensile test results

Conventional tensile testing of the Al-2% Si alloy pulled at different strain rates from 1×10^{-1} to 1×10^{-3} s^{-1} for both the as-cast condition and for 1, 2, 3, and 4 ECAP passes suggested that both the yield stress (YS) and the ultimate tensile strength (UTS) increased systematically with an increase in the number of ECAP passes. Ultimately after 4 passes, the YS and UTS of the Al-2% Si alloy at the maximum strain rate of 1×10^{-1} s^{-1} were ~250 and ~270 MPa, respectively [25].

Similarly, both the YS and UTS of the Al-2% Si alloy under similar experimental conditions were evaluated using the ball-indentation technique. The BIT results were comparable with that of conventional tensile results and they are reproduced from

Table 3. Mechanical properties measured by BIT of Al-2Si alloy processed by ECAP [25].

Alloy(Al-2Si) *condition*	UTS, MPa *at strain rate* s^{-1}			YS, MPa *at strain rate* s^{-1}		
	1×10^{-1}	1×10^{-2}	1×10^{-3}	1×10^{-1}	1×10^{-2}	1×10^{-3}
1 pass	230	218	208	212	204	192
2 pass	257	237	224	235	222	210
3 pass	272	250	239	252	240	228
4 pass	288	267	245	276	252	230

Table 4. Tensile properties of Al-2Si and Al-2Si-0.25Sc alloys.

Properties	Al-2Si 0 pass	Al-2Si-0.25Sc 0 pass	Al-2Si 4 pass	Al-2Si-0.25Sc 4 pass
Grain size, μm	~40	~25	~0.70	~0.30
YS(10^{-1} s^{-1}), MPa	59	98	250	324
UTS(10^{-1} s^{-1}), MPa	106	185	271	355

earlier work in Table 3 [25]. Since BIT requires samples of smaller dimension and with less complexity, it is suggested that it is more appropriate to use BIT samples for evaluating the mechanical properties of SPD-processed alloys. Therefore, BIT was applied to evaluate the YS and UTS of the Al-2% Si-0.25% Sc alloy. Similar observations were recorded including an increase in the UTS and YS values for up to 4 passes. The YS and UTS values at the highest strain rate $1 \times 10^{-1}s^{-1}$ were ~324 and ~355 MPa, respectively. The maximum strength values for the Al-2% Si and Al-2% Si-0.25% Sc alloys after ECAP through 4 passes for the samples pulled at the highest strain rate of 1 x 10^{-1} s^{-1} are given in Table 4.

The effect of a grain size reduction due to ECAP and Sc addition to the Al-2% Si alloy is shown in Table 4. The grain size of the cast Al-2% Si alloy was refined to 25 μm with the addition of 0.25% Sc which is very significant considering the small amount of alloy addition. It is also interesting to note that the ECAP process alone is capable of refining the grain size of the Al-2% Si alloy from 40 to 0.7 μm and also it improves the UTS value from ~106 to ~271 MPa which corresponds to an increase of ~155%. Similarly the YS value is also increased from ~59 to ~250 MPa. In the case of the Al-2% Si-0.25% Sc alloy, the grain size was reduced from 25 to 0.30 μm during ECAP through 4 passes and the UTS value was increased from ~185 to ~355 MPa which corresponds to an increase of ~92%. This type of improvement in mechanical properties due to ECAP for other alloys has also been reported [32, 33].

When the improvement of mechanical properties during ECAP of both the Al-2% Si and the Al-2% Si-0.25% Sc alloys are compared with the as-cast alloys, the Al-2% Si alloy exhibited a higher percentage improvement compared to the Al-2% Si-0.25% Sc alloy. Even though the UTS values of the Al-2% Si-0.25% Sc alloy after 4 passes is higher than for the Al-2% Si alloy after 4 passes, the incremental improvement in the UTS during mechanical working was not similar. This may be understood by considering that precipitation hardening is the most effective strengthening mechanism compared to work hardening in Al alloys. In fact, the high strength aluminum alloys come from within the precipitation hardening groups. Therefore, the results may be understood because the precipitation hardening of the Al-2% Si alloy with Al_3Sc precipitates almost doubles the UTS and after ECAP the UTS is ~3.5 times higher. In the absence of the Sc addition, the UTS is ~2.5 times that of the as-cast condition after 4 ECAP passes. It is also understood that the ultrafine-grained structure of the Al-2% Si-0.25% Sc alloy is thermally more stable by comparison with the Al-2% Si alloy due to the finer precipitates which are highly stable and introduce Zener pinning of grain boundaries and hence improved mechanical properties during service.

4. CONCLUSIONS

1. Pressing through four passes reduces the grain size from ~40 to ~0.70 μm, reduces the size of the Si particles from ~12.0 to ~1.08 μm and increases the yield stress and the ultimate tensile strength by factors of ~2 by comparison with the as-cast Al-2% Si alloy.
2. The average grain size of the as-cast Al-2% Si-0.25% Sc alloy was 25 μm which is finer than for the as-cast Al-2% Si alloy. This is due to the grain refinement effect arising from the presence of fine Al_3Sc precipitates.
3. Processing of Al-2% Si-0.25% Sc samples by ECAP showed further improvement in microstructure and tensile properties as compared to the Al-2% Si alloy after similar ECAP. The average grain size was reduced to 0.30 μm after 4 passes which was finer than for the Al-2% Si alloy after 4 passes. The four pass Al-2% Si-0.25% Sc alloy exhibited a UTS value of ~355 MPa which was ~30% higher than ~270 MPa for the four pass Al-2% Si alloy.

ACKNOWLEDGEMENTS

One of the authors (KV) is grateful to the Council of Scientific and Industrial Research (CSIR), New Delhi, Government of India and Director, National Aerospace Laboratories, Bangalore (CSIR), for deputing him to Ufa, Russia, to present this work. We sincerely thank Dr Mainak Ghosh and Ms. Mousumi Das of NML, Jamshedpur for their help in TEM and BIT studies respectively. Part of this research was conducted at the University of Southern California with support from the National Science Foundation under Grant No. DMR-0855009.

REFERENCES

[1] B. K. Prasad // *J. Mater. Sci.* **10** (1991) 867.
[2] O. Uzun, *Ph.D. Thesis* (Department of Physics, Gazi University Institute of Science and Technology, Turkey, 1998).
[3] S. Das, A. H. Yegnesvaran and P. K. Rohatgi // *J. Mater. Sci.* **22** (1987) 3173.
[4] S. Su, X. Liang, A. Moran and E. J. Lavernia // *Int. J. Rap. Sol.* **8** (1994) 161.
[5] L.A. Willey // *U.S. Patent No. 3619181;* 1971.
[6] N. Blake and M.A. Hopkins // *J Mater Sci* **20** (1985) 2861.
[7] R.R. Sawtell and C.L. Jensen // *Metall. Trans.* **21A** (1990) 421.
[8] B.A. Parker, Z.F. Zhou and P. Nolle // *J Mater Sci* **30** (1995) 452.
[9] V.G. Davydov, T.D. Rostova, V.V. Zakharov, Yu.A. Filatov and V.I. Yelagin // *Mater. Sci. Eng* **A280** (2000) 30.
[10] Yu.A. Filatov, V.I. Yelagin and V.V. Zakahrov // *Mater. Sci. Eng*. **A280** (2000) 97.
[11] S. Iathbai and P.G. Lloyd // *Acta Mater*. **50** (2002) 4275.
[12] O. Roeder, O. Schauerte, G. Lutjering and A. Gysler // *Mater. Sci. Forum* **217-222** (1996) 1835.
[13] T. Aiura, N. Sugawara and Y. Miura // *Mater. Sci. Eng.* **A280** (2000) 139.
[14] Z. Yin, Q. Pan, Y. Zhang and F. Jiang // *Mater. Sci. Eng*. **A280** (2000) 151.
[15] A.F. Norman, P.B. Prangnell and R.S. McEwen // *Acta Mater*. **46** (1998) 5715.
[16] K. Venkateswarlu, L.C. Pathak, A.K. Ray, G. Das, P.K. Verma, A. Kumar and R.N. Ghosh // *Mater. Sci. Eng*. **A383** (2004) 374.
[17] R.Z. Valiev and T.G. Langdon // *Prog. Mater. Sci.* **51** (2006) 881.
[18] R.Z. Valiev, N.A. Krasilnikov and N.K. Tsenev // *Mater. Sci. Eng*. **A137** (1991) 35.
[19] Z. Horita, T. Fujinami, M. Nemoto and T.G. Langdon, // *Metall. Mater. Trans.* **31A** (2000) 691.
[20] T.G. Langdon // *Reviews on Advanced Materials Science* **13** (2006) 6.
[21] R.Z. Valiev and T.G. Langdon // *Reviews on Advanced Materials Science* **13** (2006) 15.
[22] M. Furukawsa, Y. Iwahashi, Z. Horita, M. Nemoto and T.G. Langdon // *Mater. Sci. Eng*. **A257** (1998) 328.
[23] K. Oh-ishi, Z. Horita, M. Furukawa, M. Nemoto and T.G. Langdon // Metall. Mater. Trans. **29A** (1998) 2011.
[24] R. Lapovok, P.W.J. McKenzie, P.F. Thomson and S.L. Semiatin // *J. Mater. Sci.* 42 (2007) 1649.
[25] K. Venkateswarlu, G. Das, A.K. Pramanik, C. Xu and T.G. Langdon // *Mater. Sci. Eng.* **A427** (2006) 188.
[26] Y. Iwahashi, J. Wang, Z. Horita, M. Nemoto and T.G. Langdon // *Scripta Mater*. 35 (1996) 143.
[27] Y. Iwahashi, Z. Horita, M. Nemoto and T.G. Langdon // *Acta Mater.* **45** (1997) 4019.
[28] Y. Iwahashi, Z. Horita, M. Nemoto and T.G. Langdon // *Acta Mater.* **46** (1998) 3317.
[29] G. Das, S. Ghosh, S. Ghosh, R.N. Ghosh // *Mater. Sci. Eng. A* 408 (2005)158.

[30] G. Das, S. Ghosh and S. Ghosh // *NDTE Int*. **39** (2006) 155.

[31] Y. Nishida, H. Arima, J.C. Kim and T. Ando // *Scripta Mater*. **45** (2001) 261.

[32] Shun Cai Wang, Marco J. Starink, Nong Gao, Cheng Xu and Terence G. Langdon // *Rev. Adv. Mat. Sci.* **10** (2005) 249.

[33] Marco J. Starink, Nong Gao, Minoru Furukawa, Zenji Horita, Cheng Xu and Terence G. Langdon // *Rev. Adv. Mat. Sci.* **7** (2004) 1.